

Supplementary Information

Novel 3-(Aminomethyl)naphthoquinone Mannich Base-Platinum(IV) Complexes: Synthesis, Characterization, Electrochemical and Cytotoxic Studies

Gustavo B. da Silva,^a Amanda P. Neves,^{#,a} Maria D. Vargas,^{*,a} Wagner A. Alves,^b
José D. B. Marinho-Filho,^c Cláudia Pessoa,^c Manoel O. Moraes^c and
Letícia V. Costa-Lotufo^c

^aInstituto de Química, Universidade Federal Fluminense, Campus do Valonguinho, Centro,
24020-150 Niterói-RJ, Brazil

^bDepartamento de Química, Universidade Federal Rural do Rio de Janeiro, Campus de Seropédica,
BR-465 Km 7, 23890-000 Seropédica-RJ, Brazil

^cDepartamento de Fisiologia e Farmacologia, Centro de Ciências da Saúde,
Universidade Federal do Ceará, Centro, 60430-270 Fortaleza-CE, Brazil

Electrospray ionization mass spectroscopy (ESI-MS) spectra

ESI-MS spectra were acquired on a quadrupole time-of-flight mass spectrometer (Q-TOF spectrometer)

(Micromass, Manchester, U.K.). The mass spectrometry (MS) parameters were set to scan from 90 to 1000 m/z using positive detection. The dry gas flow was set to 50.0 L min^{-1} , the dry temperature to 120 °C and the flow injection rate to 4.0 $\mu\text{L min}^{-1}$.

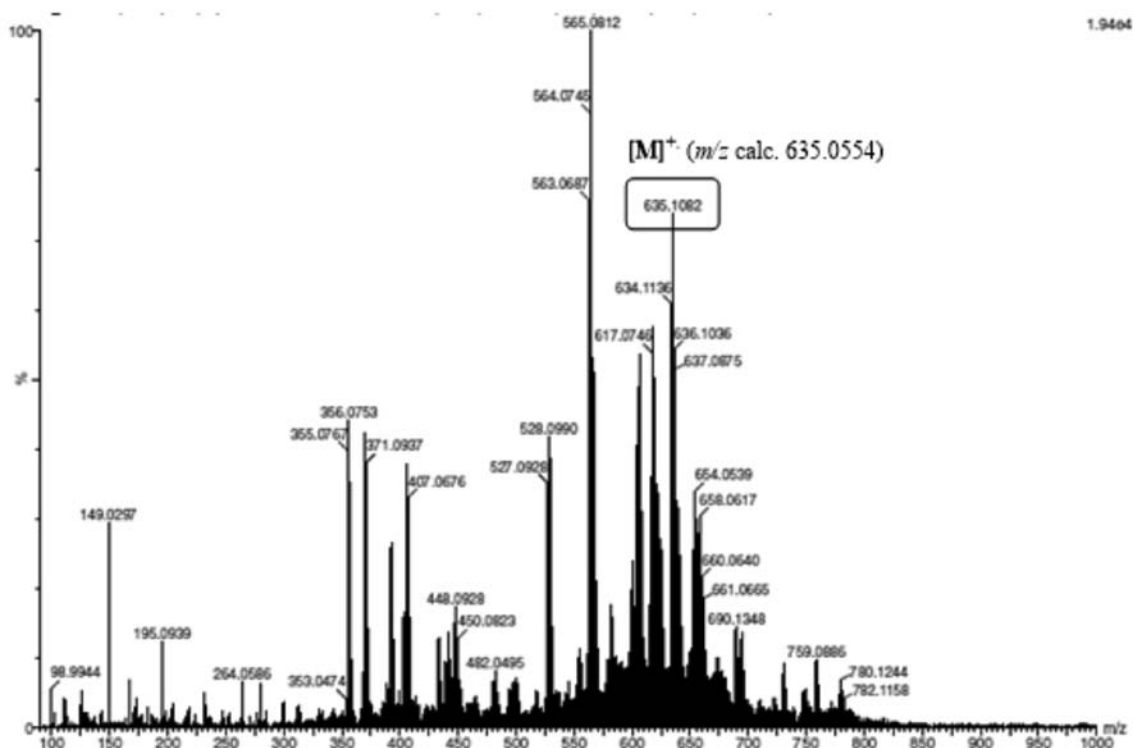


Figure S1. ESI-MS (positive mode) spectrum of 1b.

*e-mail: mdvargas@vm.uff.br

[#]Present Address: Departamento de Química, Universidade Federal Rural do Rio de Janeiro, Campus de Seropédica, BR-465 km 7, 23890-000 Seropédica-RJ, Brazil

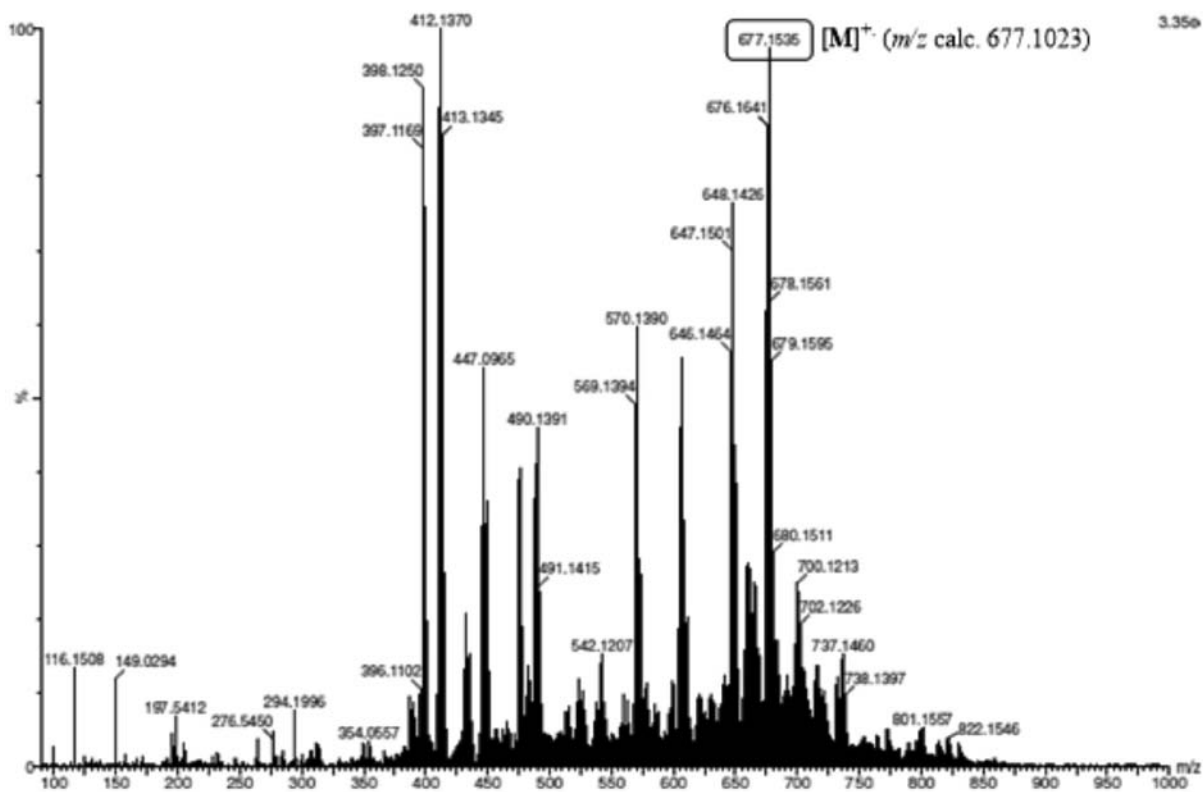


Figure S2. ESI-MS (positive mode) spectrum of 2b.

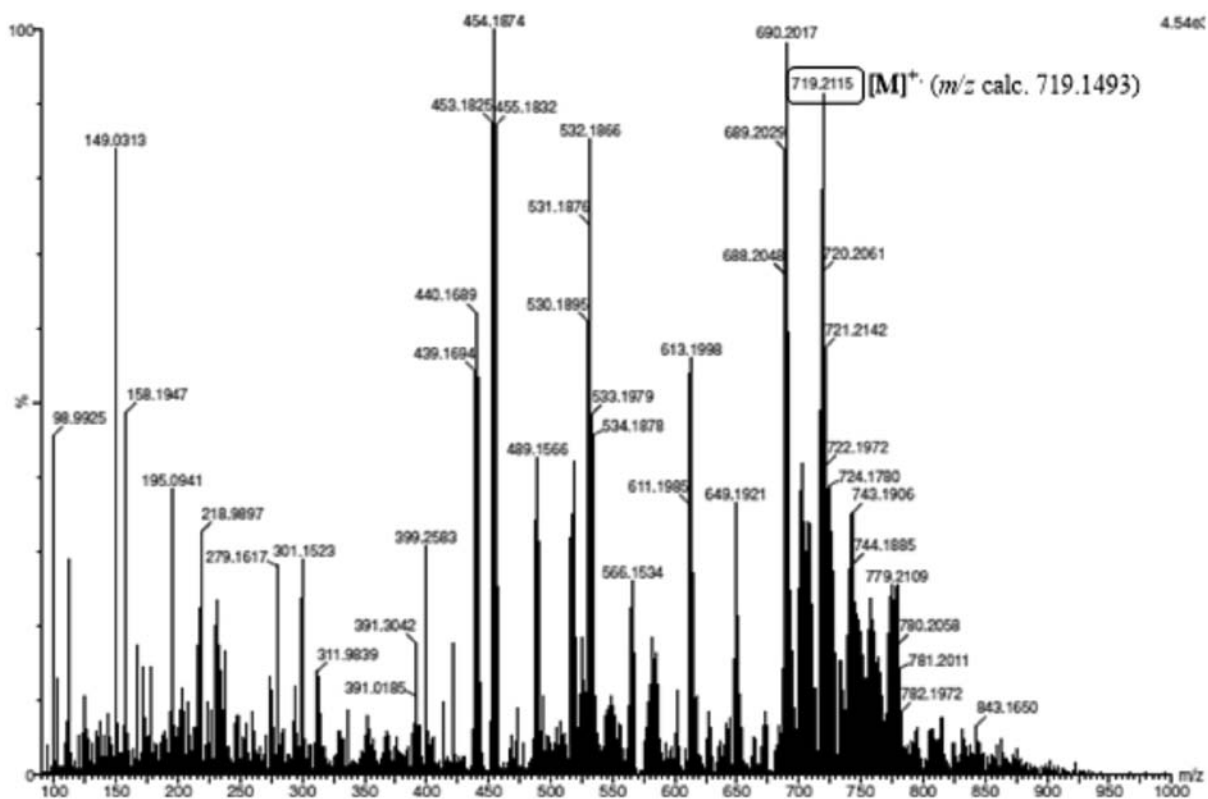


Figure S3. ESI-MS (positive mode) spectrum of 3b.

IR and Raman spectra

Infrared (IR) spectra were recorded on a Nicolet FT-IR Magna 760 spectrophotometer using CsI pellets and Raman experiments were carried out on a Bruker FT-Raman MultiRAM using the 1064 nm line of a Nd:YAG laser and a Ge detector operating at liquid nitrogen temperature.

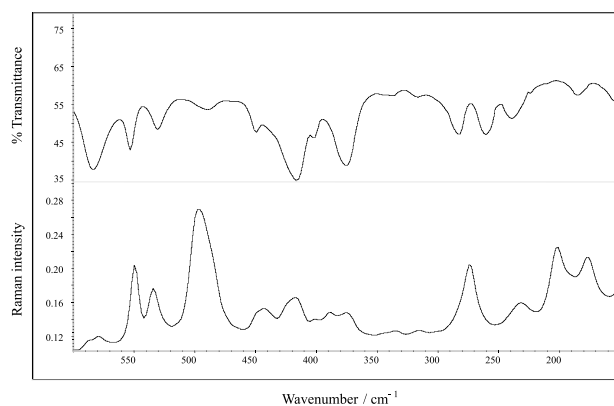


Figure S4. Far-IR (top) and Raman (bottom) spectra of **HL2**.

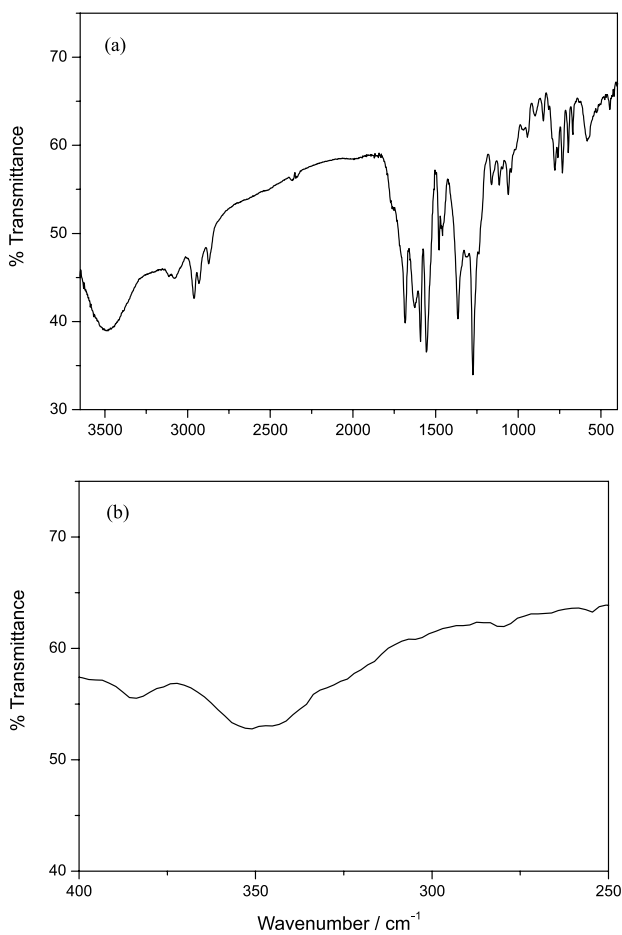


Figure S5. Middle (a) and far-IR (b) spectra of **1b**.

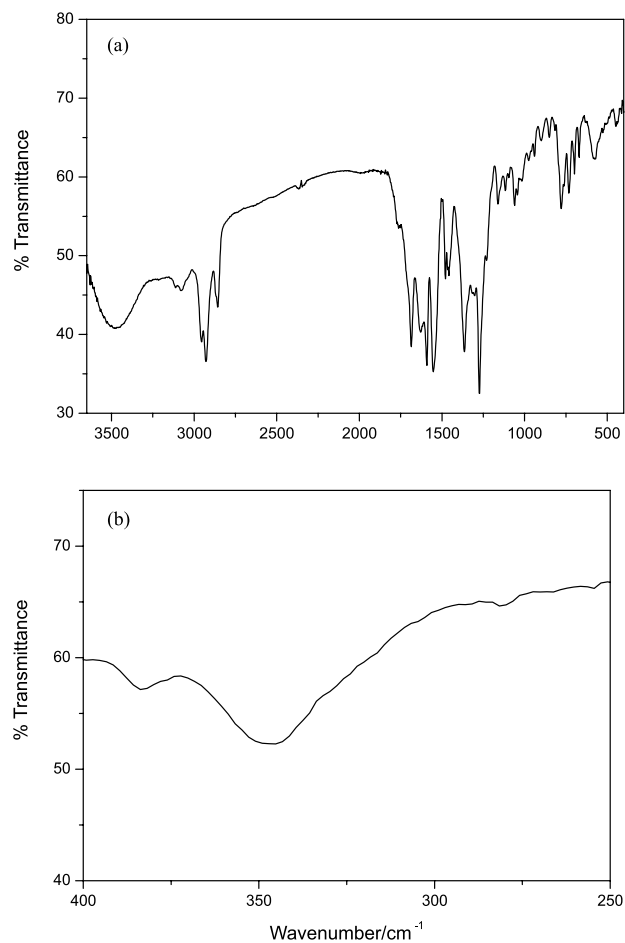


Figure S6. Middle (a) and far-IR (b) spectra of **2b**.

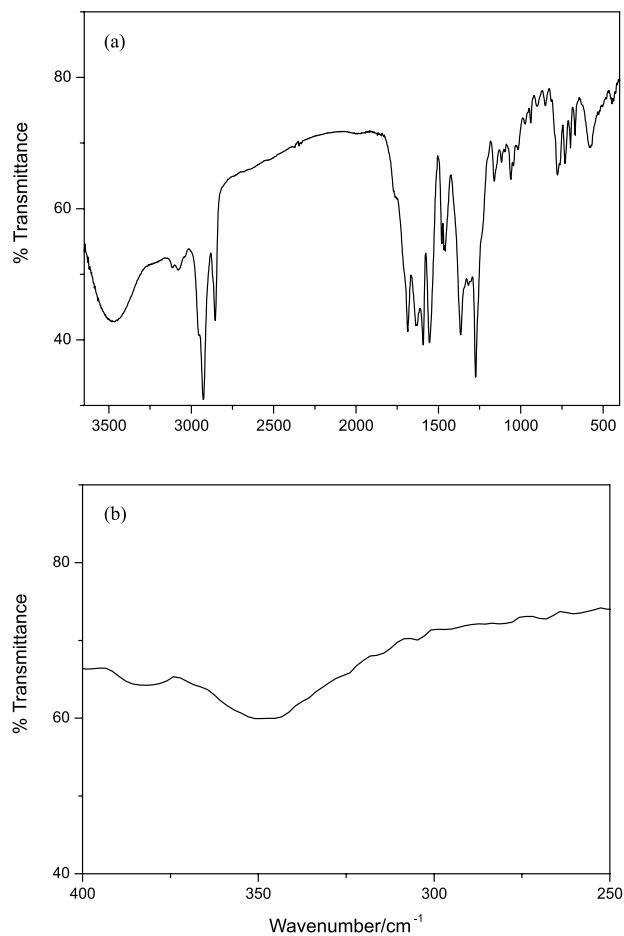


Figure S7. Middle (a) and far-IR (b) spectra of 3b.

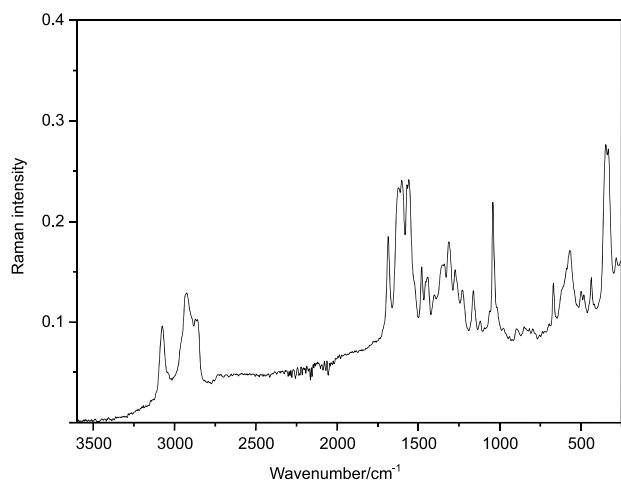


Figure S8. Raman spectrum of 2b

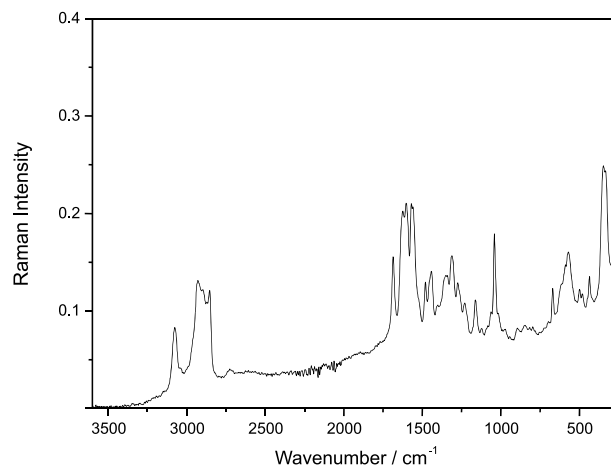


Figure S9. Raman spectrum of 3b.

Cyclic voltammetry experiments

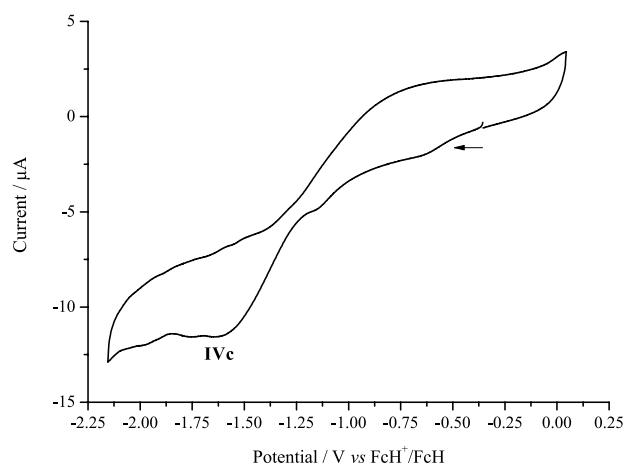


Figure S10. Cyclic voltammogram of *cis,cis,trans*-[Pt(NH₃)₂Cl₂(OH)₂] A in 0.1 mol L⁻¹ *n*-Bu₄ClO₄/MeCN obtained at 0.1 V s⁻¹ with a glassy carbon electrode, the potentials being referred to the FcH⁺/FcH.

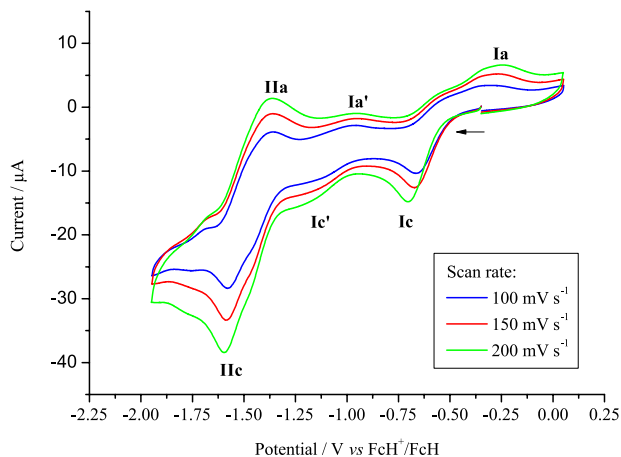


Figure S11. Cyclic voltammograms of **1a** obtained with a glassy carbon electrode (3 mm) in $0.1 \text{ mol L}^{-1} n\text{-BuNClO}_4/\text{CH}_3\text{CN}$ at different scan rates. The potential scan was initiated in the cathodic direction. The cathodic (Ic, Ic' and IIc) and anodic (Ia, Ia' and IIa) peaks are indicated.

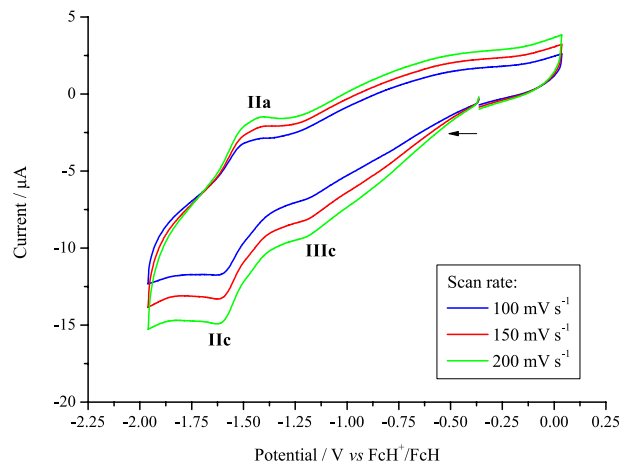


Figure S14. Cyclic voltammograms of **1b** obtained with a glassy carbon electrode (3 mm) in $0.1 \text{ mol L}^{-1} n\text{-BuNClO}_4/\text{CH}_3\text{CN}$ at different scan rates. The potential scan was initiated in the cathodic direction. The cathodic (IIc and IIIc) and anodic (IIa) peaks are indicated.

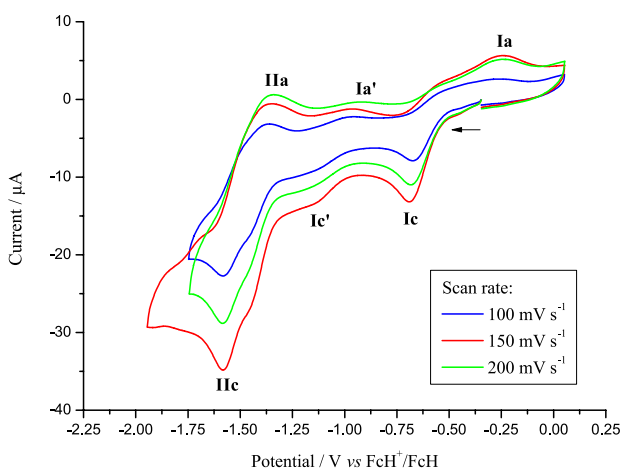


Figure S12. Cyclic voltammograms of **2a** obtained with a glassy carbon electrode (3 mm) in $0.1 \text{ mol L}^{-1} n\text{-BuNClO}_4/\text{CH}_3\text{CN}$ at different scan rates. The potential scan was initiated in the cathodic direction. The cathodic (Ic, Ic' and IIc) and anodic (Ia, Ia' and IIa) peaks are indicated.

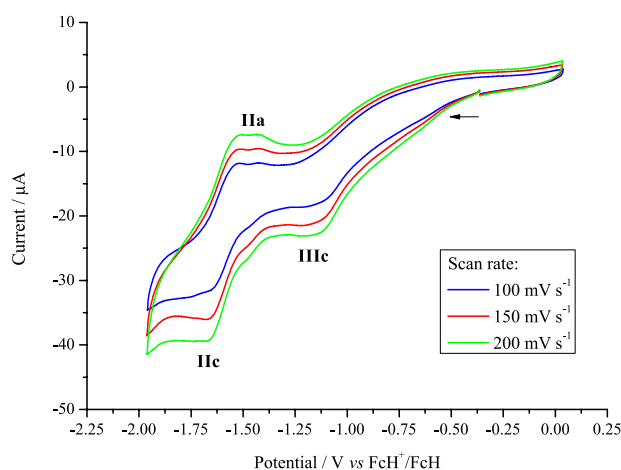


Figure S15. Cyclic voltammograms of **2b** obtained with a glassy carbon electrode (3 mm) in $0.1 \text{ mol L}^{-1} n\text{-BuNClO}_4/\text{CH}_3\text{CN}$ at different scan rates. The potential scan was initiated in the cathodic direction. The cathodic (IIc and IIIc) and anodic (IIa) peaks are indicated.

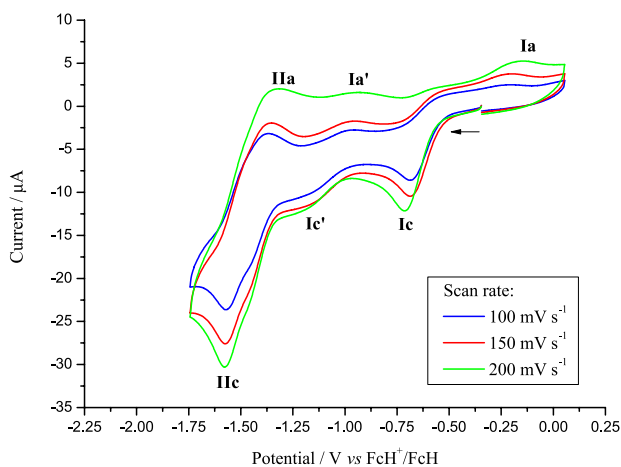


Figure S13. Cyclic voltammograms of **3a** obtained with a glassy carbon electrode (3 mm) in $0.1 \text{ mol L}^{-1} n\text{-BuNClO}_4/\text{CH}_3\text{CN}$ at different scan rates. The potential scan was initiated in the cathodic direction. The cathodic (Ic, Ic' and IIc) and anodic (Ia, Ia' and IIa) peaks are indicated.

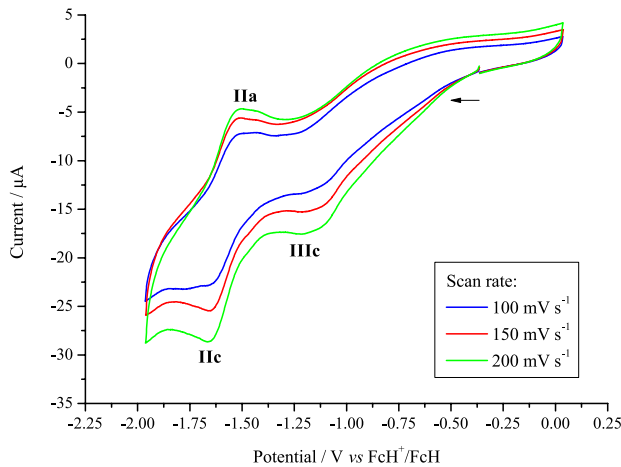


Figure S16. Cyclic voltammograms of **3b** obtained with a glassy carbon electrode (3 mm) in $0.1 \text{ mol L}^{-1} n\text{-BuNClO}_4/\text{CH}_3\text{CN}$ at different scan rates. The potential scan was initiated in the cathodic direction. The cathodic (IIc and IIIc) and anodic (IIa) peaks are indicated.

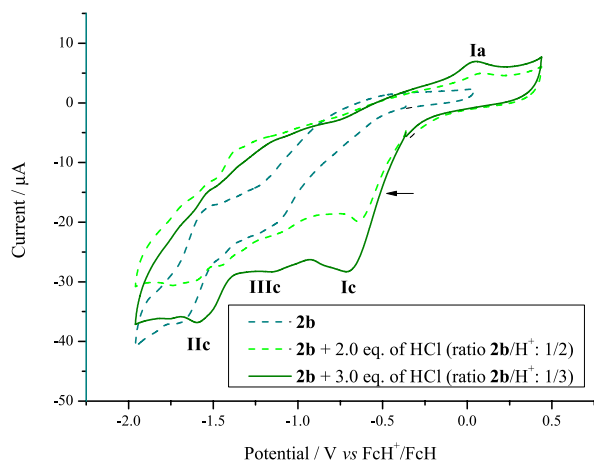


Figure S17. Cyclic voltammograms of **2b** obtained after addition of 0.05 mol L⁻¹ HCl (2 and 3 equivalent), with a glassy carbon electrode (3 mm) in 0.1 mol L⁻¹ *n*-Bu₄NClO₄/CH₃CN. The potential scan was initiated in the cathodic direction. The cathodic (**Ic**, **IIc** and **IIIc**) and anodic (**Ia**) peaks are indicated.

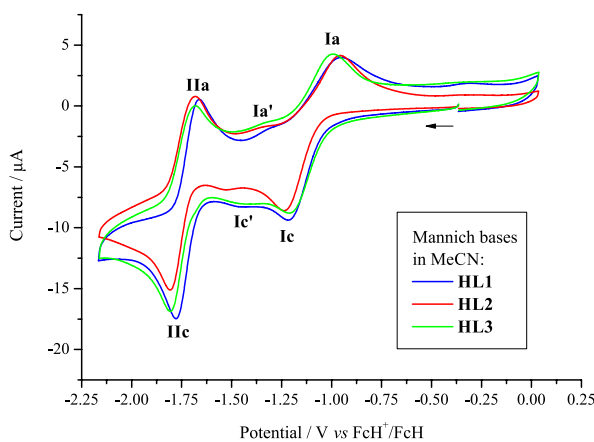


Figure S18. Cyclic voltammograms of **HL1-HL3** obtained with a glassy carbon electrode (3 mm) in 0.1 mol L⁻¹ *n*-Bu₄NClO₄/CH₃CN. The potential scan was initiated in the cathodic direction. The cathodic (**Ic**, **Ic'** and **IIc**) and anodic (**Ia**, **Ia'** and **IIa**) peaks are indicated.

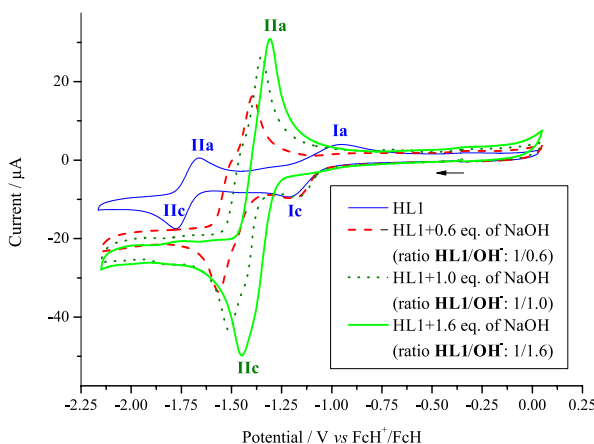


Figure S19. Cyclic voltammograms of **HL1** obtained after addition of different amounts of 0.02 mol L⁻¹ NaOH_(aq) with a glassy carbon electrode (3 mm) in 0.1 mol L⁻¹ *n*-Bu₄NClO₄/CH₃CN. The potential scan was initiated in the cathodic direction. The cathodic (**Ic** and **IIc**) and anodic (**Ia** and **IIa**) peaks are indicated.

To avoid the presence of water, which strongly affects the CV profile, the same experiment was performed using the proton sponge DBU (1,8-diazabicyclo[5.4.0]undec-7-ene). After addition of 1.0 equivalent of DBU to the MeCN solutions of HL1-3 the CVs showed the presence of two redox processes, the redox pair **Ic/Ia** being shifted to more negative potential with respect to that in pure MeCN. This result indicates that this solvent does not stabilize the semiquinone as efficiently as water. Indeed, after addition of the same amount of water used in the experiment with aqueous NaOH (400 μL) to the MeCN solution of HL1-3 (5 mL, i.e., 7.4% H₂O in MeCN) a single pair was observed.

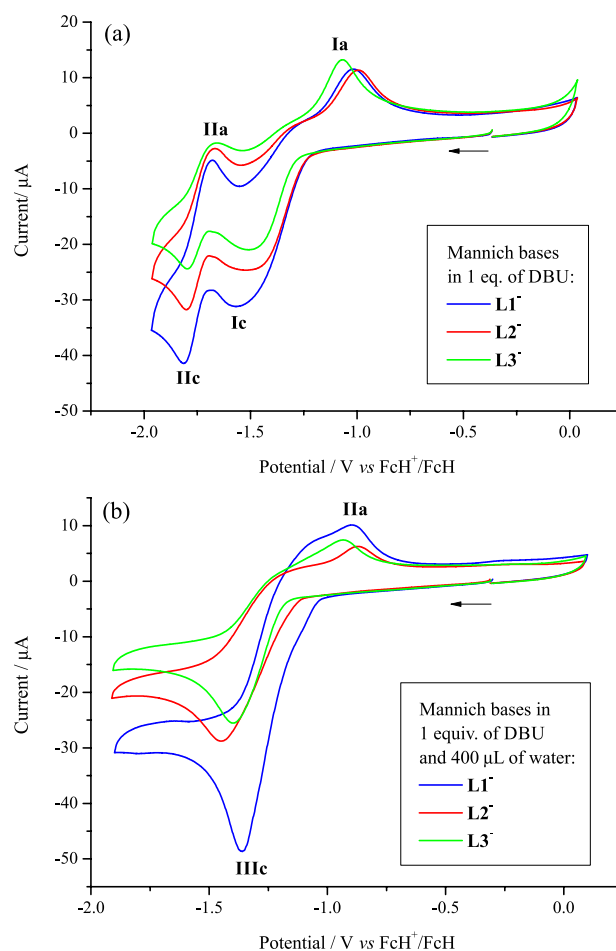


Figure S20. Cyclic voltammograms of **L1-L3** obtained with a glassy carbon electrode (3 mm) in 0.1 mol L⁻¹ *n*-Bu₄NClO₄/CH₃CN: (a) after addition of 1 equiv. DBU (0.05 mol L⁻¹ in CH₃CN); (b) after addition of H₂O (400 μL) to the previous solution. The potential scan was initiated in the cathodic direction. The cathodic (**Ic**, **Ic'** and **IIc**) and anodic (**Ia**, **Ia'** and **IIa**) peaks are indicated.

All cyclic voltammograms were also performed in CH₂Cl₂ + Bu₄NClO₄. The electrochemical behavior was similar to that observed in MeCN (Figures S21-S29 and Table S1).

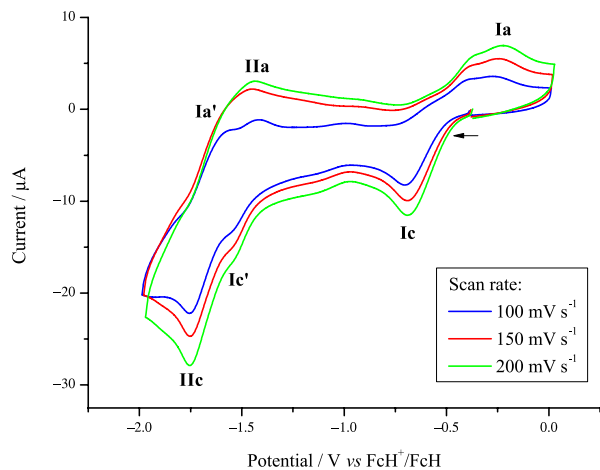


Figure S21. Cyclic voltammograms of **1a** obtained with a glassy carbon electrode (3 mm) in $0.1 \text{ mol L}^{-1} n\text{-BuNClO}_4/\text{CH}_2\text{Cl}_2$. The potential scan was initiated in the cathodic direction. The cathodic (**Ic**, **Ic'** and **IIc**) and anodic (**Ia**, **Ia'** and **IIa**) peaks are indicated.

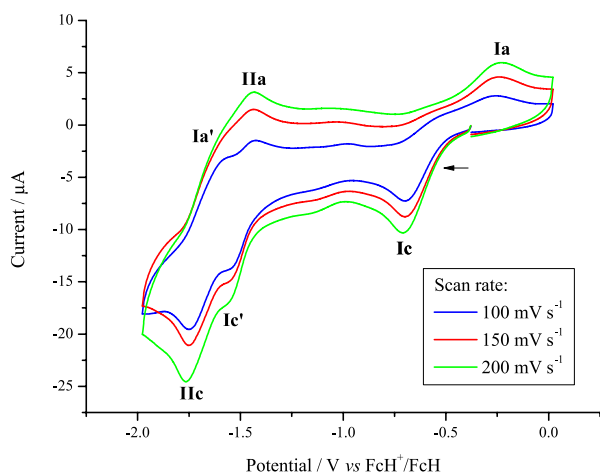


Figure S22. Cyclic voltammograms of **2a** obtained with a glassy carbon electrode (3 mm) in $0.1 \text{ mol L}^{-1} n\text{-BuNClO}_4/\text{CH}_2\text{Cl}_2$. The potential scan was initiated in the cathodic direction. The cathodic (**Ic**, **Ic'** and **IIc**) and anodic (**Ia**, **Ia'** and **IIa**) peaks are indicated.

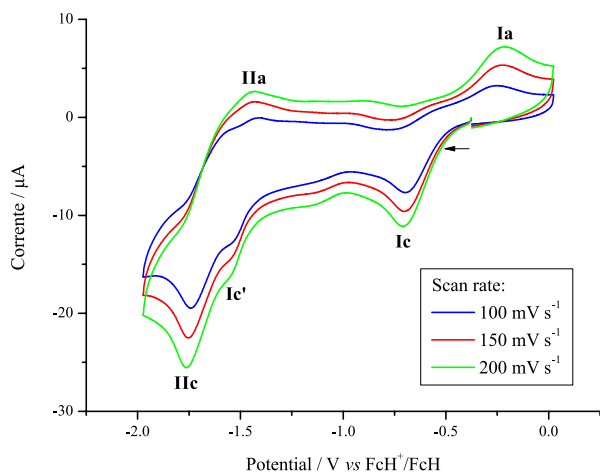


Figure S23. Cyclic voltammograms of **3a** obtained with a glassy carbon electrode (3 mm) in $0.1 \text{ mol L}^{-1} n\text{-BuNClO}_4/\text{CH}_2\text{Cl}_2$. The potential scan was initiated in the cathodic direction. The cathodic (**Ic**, **Ic'** and **IIc**) and anodic (**Ia** and **IIa**) peaks are indicated.

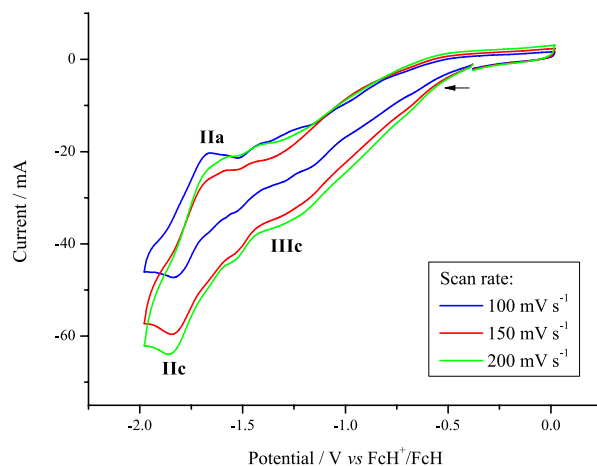


Figure S24. Cyclic voltammograms of **1b** obtained with a glassy carbon electrode (3 mm) in $0.1 \text{ mol L}^{-1} n\text{-BuNClO}_4/\text{CH}_2\text{Cl}_2$. The potential scan was initiated in the cathodic direction. The cathodic (**IIc** and **IIIc**) and anodic (**IIa**) peaks are indicated.

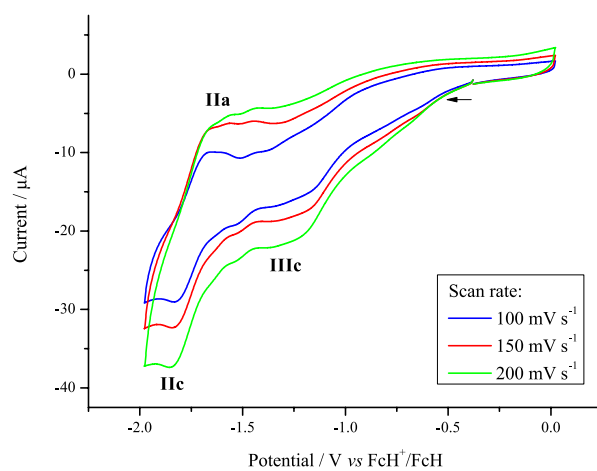


Figure S25. Cyclic voltammograms of **2b** obtained with a glassy carbon electrode (3 mm) in $0.1 \text{ mol L}^{-1} n\text{-BuNClO}_4/\text{CH}_2\text{Cl}_2$. The potential scan was initiated in the cathodic direction. The cathodic (**IIc** and **IIIc**) and anodic (**IIa**) peaks are indicated.

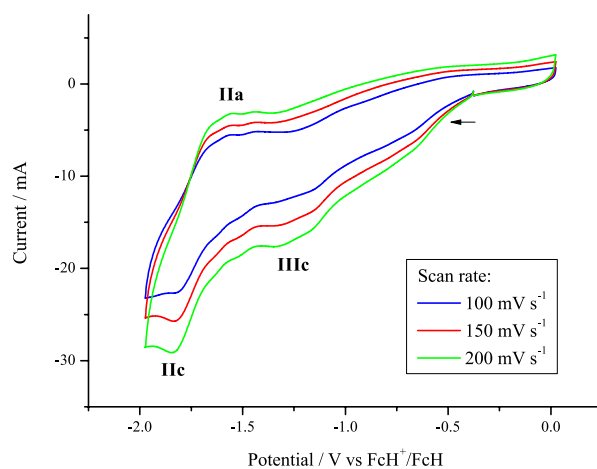


Figure S26. Cyclic voltammograms of **3b** obtained with a glassy carbon electrode (3 mm) in $0.1 \text{ mol L}^{-1} n\text{-BuNClO}_4/\text{CH}_2\text{Cl}_2$. The potential scan was initiated in the cathodic direction. The cathodic (**IIc** and **IIIc**) and anodic (**IIa**) peaks are indicated.

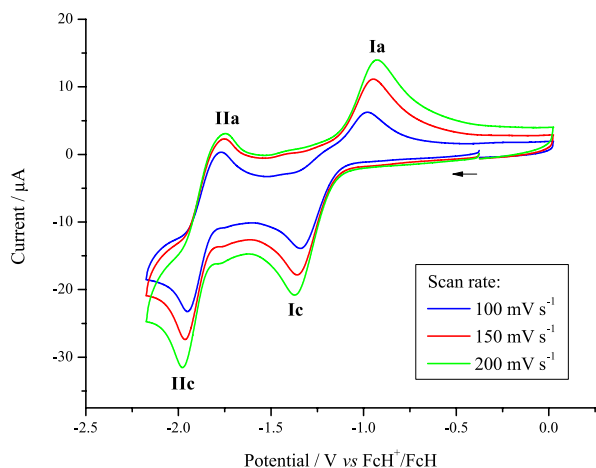


Figure S27. Cyclic voltammograms of **HL1** obtained with a glassy carbon electrode (3 mm) in 0.1 mol L⁻¹ *n*-Bu₄NClO₄/CH₂Cl₂. The potential scan was initiated in the cathodic direction. The cathodic (**Ic** and **IIc**) and anodic (**Ia** and **IIa**) peaks are indicated.

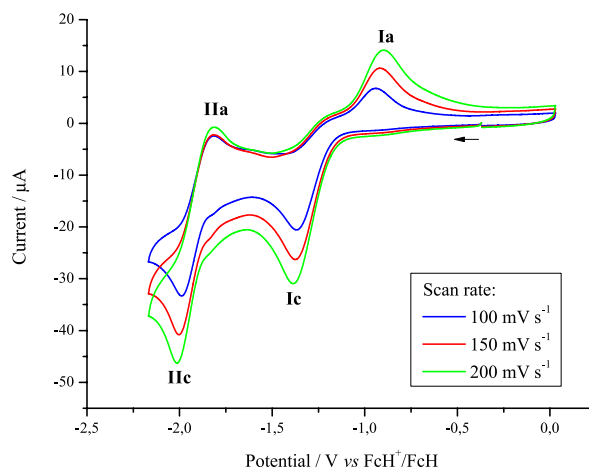


Figure S29. Cyclic voltammograms of **HL3** obtained with a glassy carbon electrode (3 mm) in 0.1 mol L⁻¹ *n*-Bu₄NClO₄/CH₂Cl₂. The potential scan was initiated in the cathodic direction. The cathodic (**Ic** and **IIc**) and anodic (**Ia** and **IIa**) peaks are indicated.

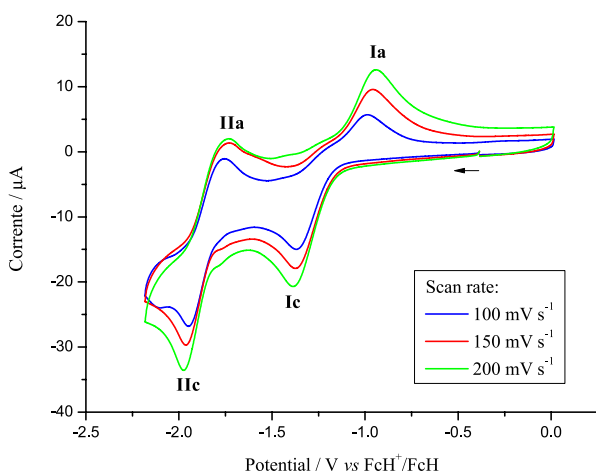


Figure S28. Cyclic voltammograms of **HL2** obtained with a glassy carbon electrode (3 mm) in 0.1 mol L⁻¹ *n*-Bu₄NClO₄/CH₂Cl₂. The potential scan was initiated in the cathodic direction. The cathodic (**Ic** and **IIc**) and anodic (**Ia** and **IIa**) peaks are indicated.

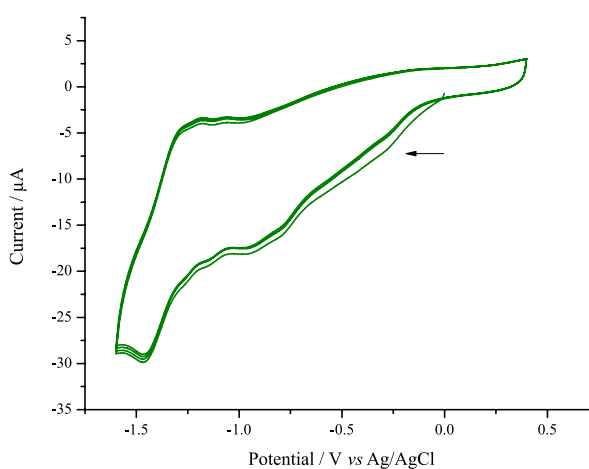


Figure S30. Successive cyclic voltammograms of **3b** obtained with a glassy carbon electrode (3 mm) in 0.1 mol L⁻¹ *n*-Bu₄NClO₄/CH₂Cl₂. The potential scan was initiated in the cathodic direction.

Table S1. Electrochemical data for: **HL1-HL3**, (b) **1a-3a** and (c) **1a-3a**, obtained in CH₂Cl₂ + 0.1 mol L⁻¹ *n*-Bu₄NClO₄ at a scan rate of 100 mV s⁻¹, at 25 °C.

E _p / V	Compounds								
	HL1	HL2	HL3	1a	2a	3a	1b	2b	3b
Ep _{Ic}	-1.34	-1.37	-1.37	-0.70	-0.70	-0.70	–	–	–
Ep _{Ic'}	–	–	–	-1.56	-1.57	-1.54	–	–	–
Ep _{IIc}	-1.95	-1.95	-1.99	-1.76	-1.75	-1.74	-1.84	-1.84	-1.83
Ep _{Ia}	-0.98	-0.99	-0.94	-0.27	-0.25	-0.25	–	–	–
Ep _{IIa}	-1.76	-1.76	-1.82	-1.42	-1.43	-1.41	-1.66	-1.63	-1.56
Ep _{IIIc}	–	–	–	–	–	–	-1.29	-1.30	-1.32
ΔEp _I	0.36	0.38	0.43	0.43	0.45	0.45	–	–	–
ΔEp _{II}	0.19	0.19	0.17	0.34	0.32	0.33	0.18	0.21	0.27

Data from voltammetric experiments in an cathodic scan; potential values are reported vs. FcH⁺/FcH.